Table 1
Immunoconjugates in American Society of Clinical Oncology (ASCO) 2011.

Name	Target molecule	Payload	Cancer	Clinical stage	Supplement
^{131}I-chTNT-1/b	DNA/Histon H1	^{131}I	Glioma	P2	Convection enhanced
NGR-hTNF	CD13	TNF	Ovary	P2	+ Doxorubicin
Ac-lintuzumab	CD33	^{225}Actinium	AML	P2	RadioactiveT1/2 10 days
PSMA-ADC	PSMA	MMAE	Prostate	P1	4 MMAE/Ab
EC145	Folate	Deacetylvinblastine	Ovary	r-P2	Doxil vs. D/EC145
IMGN901	CD56	Maytasinoid	Multiple myeloma	P1	+ Lenaliomide/Dexa
EMD273066	EpCAM	IL2	Solid tumor	P1b	+ Cyclophosphamide
SGN-75	CD70	MMAE	Renal, NHL	P1	4.5 mg/kg/3w
CMC544	CD22	Calicheamycin	ALL	P1	
^{177}Lu-J591	PSMA	177Lu	Prostate	r-P2	^{177}Lu-J591b vs. ^{111}I-J591
Myelotag	CD33	Calicheamycin	AML	P2	Cytarabine, fludarabine
SGN-35	CD30	MMAe	HL	P2	1.8 mg/kg/3w
^{131}ILI9SIR	Tenascin-c	^{131}I	NHL	P1/2	2.05 GBq/m^2
T-DM1	HER2	DM1	Breast	P2	plts
T-DM1	HER2	DM1	Breast	P3	1st line
T-DM1	HER2	DM1	Breast	P3	Previous chemo. Trastuzumab/Taxotere

However, the use of HMW agents presents a dilemma for cancer therapy because the very properties that favor their high accumulation in the lesion also cause low diffusion of these macromolecules within a tumor [15]. Most human solid tumors possess abundant stroma that prevents immunoconjugate diffusion and, consequently, becomes a barrier preventing immunoconjugate from directly attacking cancer cells [15–18].

2. Success and failure of active targeting

Recent successful examples of immunoconjugates include anti-CD33 antibody-calicheamicin conjugate for acute myeloid leukemia and radiolabeled anti-CD20 mAbs for B-cell non-Hodgkin's lymphoma treatment [19]. On the other hand, in most human solid tumors, there are abundant stroma that prevents mAb diffusion and, consequently, becomes a barrier preventing mAb from directly attacking cancer cells. In fact, immunoconjugate therapies for common solid tumors (e.g., colorectal, lung and pancreatic cancers) have not yet proved successful in clinical practice because of heterogeneity of target antigens and low uptake and retention of chemotherapeutic drugs in these types of cancer (Fig. 1B). This contrasts with the results seen in treatment of human hematologic malignancies and of tumor xenografts in mice, which usually have less interstitial tissue within the neoplasm [19]. The kinetics of drug distribution within tumors are considered to be functions of interstitial conductivity, which is determined by the quantity and density of the extracellular matrix (ECM e.g., proteoglycan, fibronectin) and fibrosis (e.g., collagen fiber) in the stroma [15–18]. Such compact assembles of various tissue constituents in solid tumors cause reduced drug penetration and also act as a stromal barrier to prevent the diffusion of mAbs (HMW proteins) [20,21].

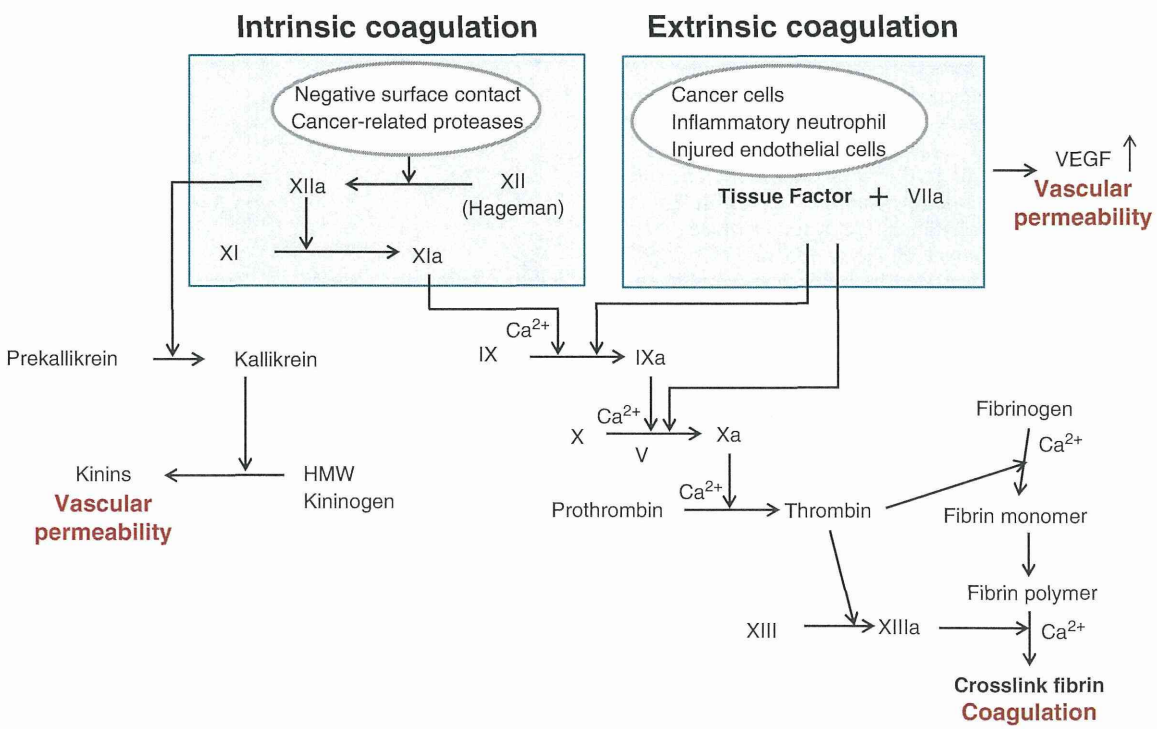

Fig. 3. Cancer and blood coagulation. Both intrinsic and extrinsic coagulation pathway may be involved in tumor vascular permeability.

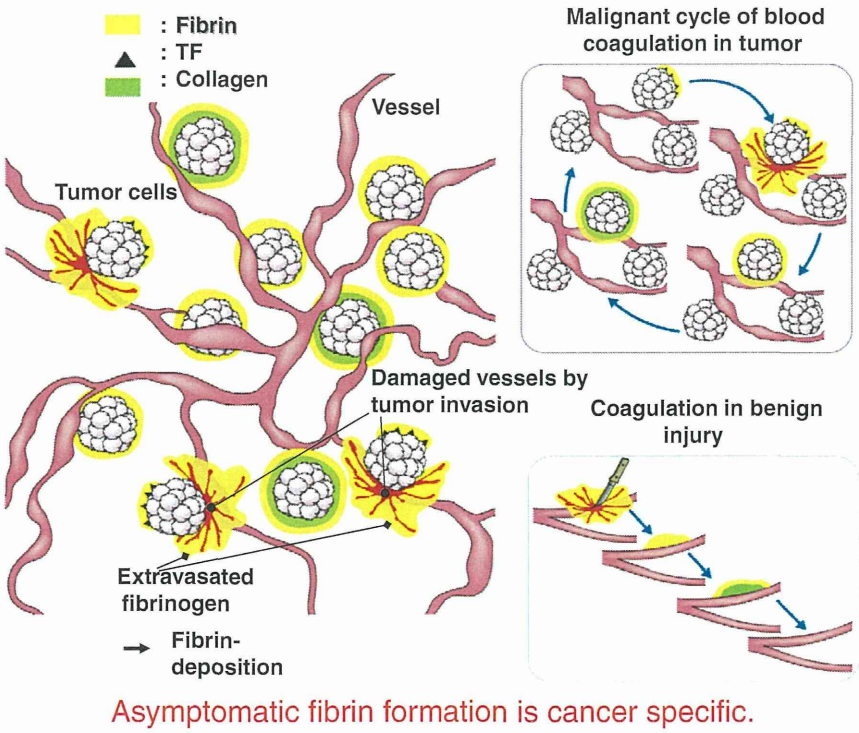

Fig. 4. Diagram of the 'malignant cycle of blood coagulation' in cancer tissue. Although the tissue factor on tumor cells may cause fibrin clot formation, most fibrin clots occur when and where fibrinogen leaks from a damaged vessel wall caused by tumor cell invasion. Fibrin clots are subsequently replaced by collagenous fibers. The malignant cycle of blood coagulation consists of four steps, namely (1) tumor cell invasion into vessel; (2) hemorrhage; (3) fibrin clot formation; and (4) replacement with collagenous tissue. There are many points in common between cancer stroma and wound healing. The absolute difference between cancer stroma and wound healing is that such conditions in cancer last for as long as cancer cells survive.

3. Cancer stroma and blood coagulation

The increased tumor vascular permeability is the most important event for the EPR effect. At the time we proposed the EPR effect, we also succeeded in purifying two types of kinin (bradykinin and hydroxyprolyl^3-bradykinin) from the ascitic fluid of a patient with gastric cancer [1,22].

We also clarified that this kinin generation system was triggered by the activated Hageman factor, an intrinsic coagulation factor XII [23].

Meanwhile, Dvorak et al. discovered that vascular permeability factor (VPF) was involved in tumor vascular permeability [24]. Later, it was found that VPF was identical to vascular endothelial growth factor (VEGF) [25]. Recently, an extrinsic coagulation factor, namely a tissue factor (TF), appeared to activate VEGF production [26]. So, both intrinsic and extrinsic coagulation factors may be involved in tumor vascular permeability as well as tumor-induced blood coagulation (Fig. 3).

In the 19th century, French surgeon Armand Trousseau described thrombophlebitis in patients with stomach cancer for the first time

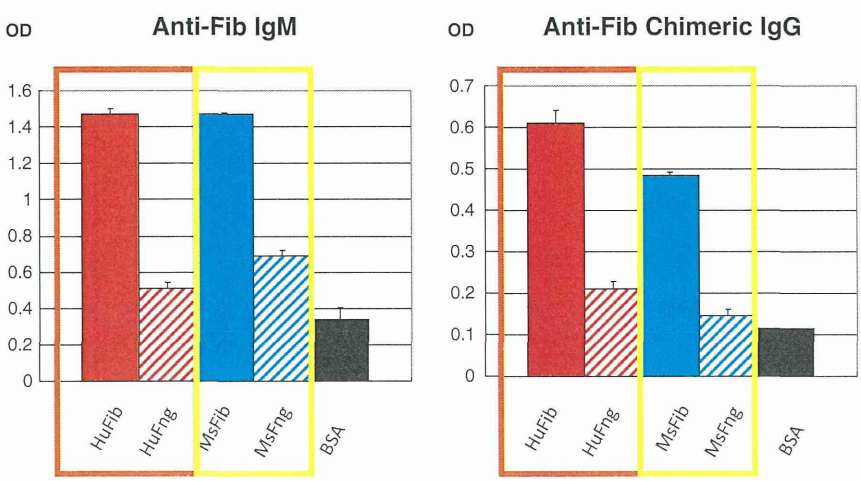

Fig. 5. Anti-fibrin IgM and its chimeric IgG recognize both human and mouse fibrin but not their fibrinogen. ELISA showed that anti-fibrin (Fib) IgM and its chimeric IgG recognize both human (Hu) and mouse (Ms) fibrin but not their fibrinogen (Fng). OD, optimal density [29].

[27]. Today, a large body of clinical evidence supports the conclusion that abnormal coagulation occurs in a variety of cancer patients [28]. It is now known that TF is highly expressed on the surface of almost all human tumor cells and alternatively spliced soluble TF is also produced by many types of tumor [26]. Therefore, TF may be involved in tumor related abnormal blood coagulation.

Above all, any malignant tumor can erode the surrounding normal tissue, and the more erosive types of cancer have more destructive actions. If these cancer clusters erode adjacent normal or tumor vessels, microscopic haemorrhage may occur at any place and at any time within or adjacent to cancer tissues, and fibrin clots immediately form in situ to stop the bleeding. The fibrin clots are subsequently replaced by collagenous stroma in a process similar to that in normal wound healing and other non-malignant diseases. Fibrin clots formation in non-malignant disorders such as cardiac infarction, brain infarction, injuries, and active rheumatoid arthritis should form only at the onset or active state of disease and subsequently disappear by plasmin digestion or replacement with collagen within a few weeks and is accompanied by some symptoms. On the other hand, the fibrin clot formation in cancer lasts for as long as the cancer cells survive in the body and occurs silently. Therefore, we call this 'malignant cycle of blood coagulation' (Fig. 4). In fact, tumor invasion and metastasis progress without symptoms (which is why imaging instruments are needed). When any symptoms accompanying cancer such as pain, intestinal obstruction, or macroscopic bleeding occur, the cancer is likely to involve sensory nerves and destruction of bones and larger blood vessels, and to occupy the whole lumen of a particular place of the intestine. Usually, patients with an advanced stage of cancer receive chemotherapy and it is worth noting that oncologists never treat such patients if they suffer from existing acute thrombotic complications, bleeding by injury, or active inflammation. Therefore, we conclude that growth factors and tyrosine kinases never become tumor-specific molecules but that fibrin clots in cancer tissues of patients who can receive chemotherapy are actually tumor-specific [29].

4. Monoclonal antibodies targeting cancer stroma

Although there are a few papers describing tumor stromal targeting using immunoconjugates, the target molecule was still a surface antigen on cells in tumor stroma, or the ECM (proteoglycan, fibronectin) was used for targeting the tumor vascular endothelial cell [30,31]. The principle of our strategy is that our newly developed immunoconjugates selectively extravasated from leaky tumor vessels, bound to the extracellular molecules in the stroma and created a scaffold from which effective sustained release of the LMW ACA occurred. This free LMW ACA can easily reach the cancer cells by diffusion through the stroma barrier. To date we have developed mAbs against collagen 4 [32], fibrin (not fibrinogen) [29], and TF that are abundantly found in the stroma of solid tumors, especially invasive tumors. In the case of anti-fibrin mAb, following extensive screening using two ELISA sets, one for human fibrinogen (physiologically existing precursor of fibrin), the other for human fibrin (being only formed at several abnormal conditions), we successfully developed a mAb that reacted only with human fibrin, not with human fibrinogen. However, since the obtained mAb was IgM, it was converted into human IgG format for clinical application using an antibody engineering technique. Another advantage of the anti-fibrin IgM and the chimeric IgG was that they cross-reacted with mouse fibrin but not with mouse fibrinogen (Fig. 5).

5. Drug design, anti-tumor activity, and PK study of immunoconjugates

5.1. Anti-mouse collagen 4 mAb conjugated with SN-38 in human pancreatic tumor xenografts

SN-38 is a topoisomerase 1 inhibitor, and an active component of CPT-11 which is used clinically for colorectal, lung and other cancers. For the mAb conjugation to phenol-OH in SN-38, an ester bond was

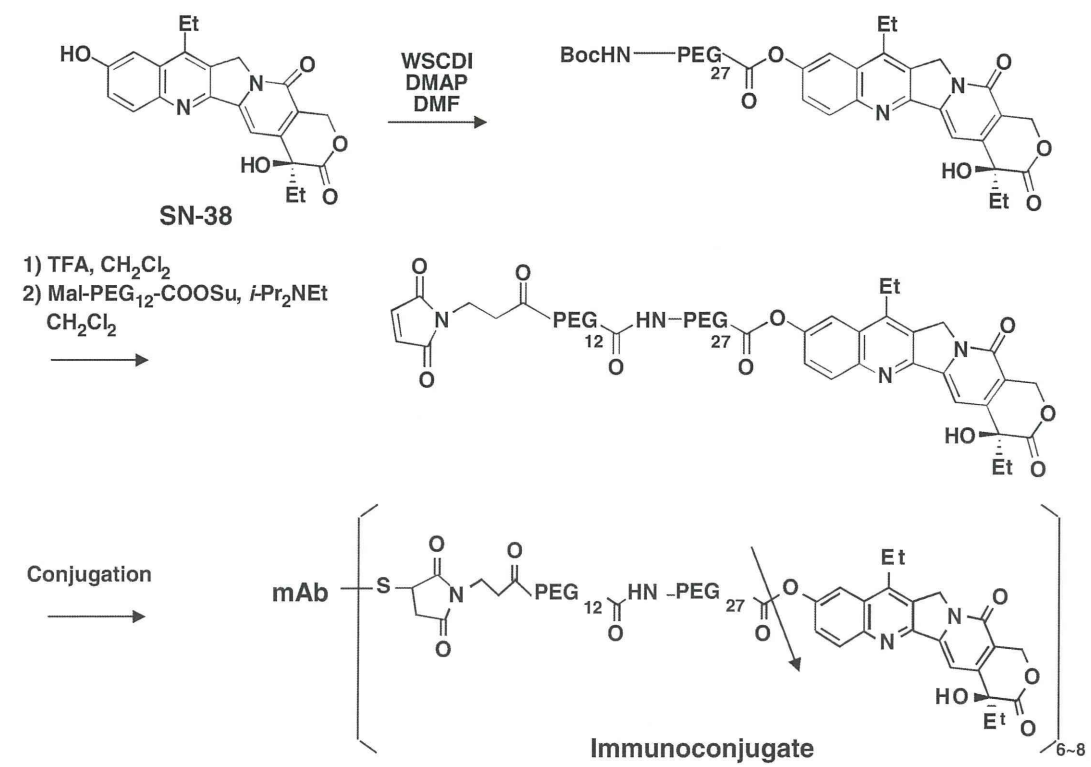

Fig. 6. Structure and drug-release of anti-mouse collagen 4 immunoconjugate. Synthetic scheme of the immunoconjugate. The arrow indicates the cleavage site for releasing free active SN-38. PEG, Polyethylene glycol [32].

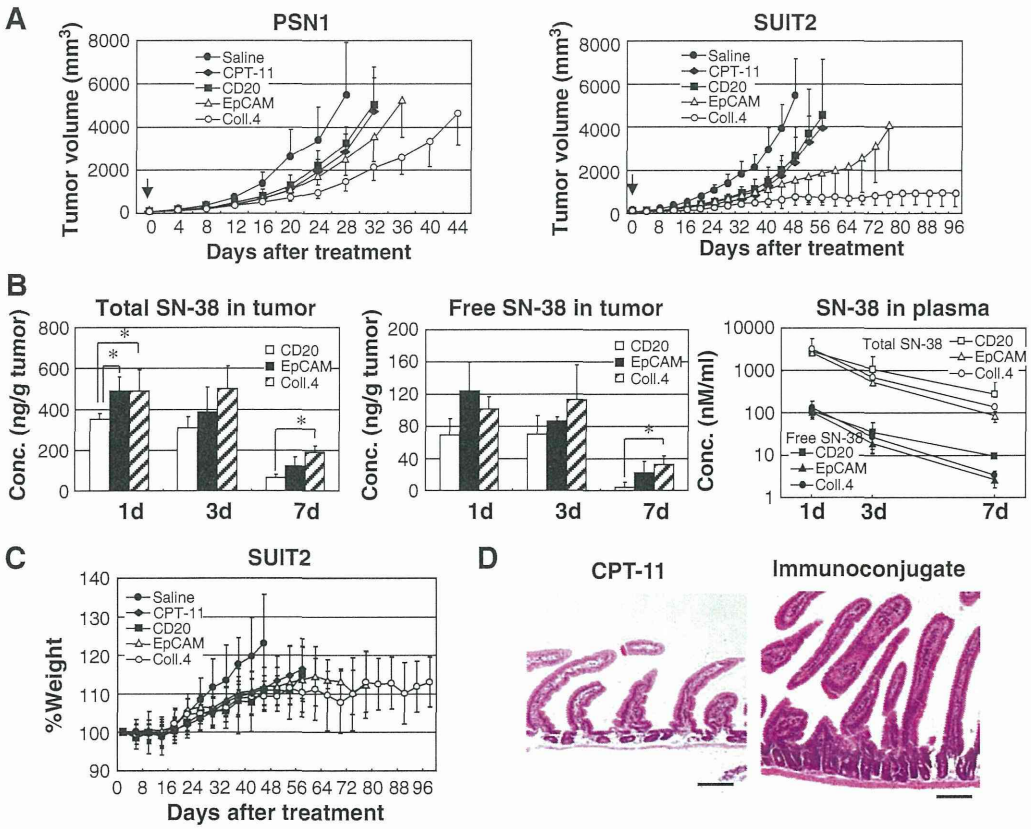

Fig. 7. Anti-tumor effects, pharmacokinetics and drug toxicities of anti-CD20, EpCAM and collagen 4 immunoconjugates. (A) Anti-tumor activities in vivo were examined. In animal models of PSN1 and SUIT2, the 3 immunoconjugates or saline as control, were administered to separate groups of mice by intravenous bolus injection on day. Arrows indicate day of administration and the curves illustrate the effects of the treatments on tumor size. $P<0.05$ (Saline or CD20 vs. EpCAM in PSN1), $P<0.01$ (Saline vs. CPT11 or EpCAM in PSN1, CPT11 or CD20 vs. EpCAM in SUIT2), $P<0.001$ (Saline vs. CPT11 or CD20 or EpCAM in SUIT2, Saline or CPT11 or CD20 or EpCAM vs. Collagen 4 in PSN1 or SUIT2). Bar = SD. (B) Tumor concentrations of total (bound and unbound) SN-38 (upper) and free (unbound) SN-38 (middle), and plasma concentrations (lower) were determined using HPLC analysis. The concentrations on days 1, 3 and 7 are shown. $^{*}P<0.05$, Bar = SD. (C) Changes in the % body weight of saline, CPT-11, CD20, EpCAM and Collagen 4 in the same treated SUIT2 group (A) were shown Bar = SD. (D) Pathologic mucosal change of jejunum from mouse treated with CPT11 (upper) or anti-collagen 4 immunoconjugate (lower). Scale bar: 1 mm [32].

selected. In our design, polyethylene glycol (PEG) was combined close to the bond (Fig. 6). PEG is known to evade non-specific capture by RES. The steric structure around the bond protects against immunoconjugate degradation in the blood. PEG has already been used for this purpose [2,3,11,33]. The drug (SN-38)/mAb ratio (the number of drugs attached to a mAb) of each immunoconjugate ranged from 6.7 to 8.4.

Anti-tumor activities of immunoconjugates with ester bond SN-38 were evaluated in mice bearing human pancreatic tumor genografts. CPT-11 and three immunoconjugates showed significant anti-tumor activities compared to results in mice treated with saline, in mice bearing either PSN1 (EpCAM positive and stroma poor) or SUIT2 (EpCAM positive and stroma rich) tumors. In SUIT2 tumors, while the tumor continued to increase in mice treated with CPT-11, anti-CD20 immunoconjugate (as a non-specific control) and anti-EpCAM immunoconjugate, the tumor treated in mice with anti-collagen 4 immunoconjugate stopped growing by about one month and never resumed up to 3 months (Fig. 7A). In mice bearing PSN1 tumors (stroma poor), differences were present but less marked. Thus, anti-collagen 4 SN-38-immunoconjugate exerted the most potent antitumor activity as compared with, anti-CD20 or anti-EpCAM immunoconjugates, and CPT-11 (Fig. 7A). In both tumor models, anti-EpCAM immunoconjugate exerted superior antitumor effect compared to CPT-11 and anti-CD20 immunoconjugate, but inferior anti-tumor effect to anti-collagen 4 SN38-immunoconjugate.

Significantly higher concentrations of free and total SN-38 were detected in tumor tissues of mice treated with the anti-collagen 4 immunoconjugate compared to the anti-CD20 immunoconjugate (Fig. 7B). The tumor concentration of free and total SN-38 treated with anti-EpCAM immunoconjugate was intermediate among them, but not significant (Fig. 7B). There was no significant difference in body weight changes among saline groups, CPT-11 and immunoconjugate groups (Fig. 7C). In the small intestinal mucosa of mice, widespread villous atrophy and decreased crypt density were observed by the treatment of free unbound CPT-11 which is well-known to have severe intestinal toxicity in clinics. On the other hand, the small intestinal mucosa of mice in groups treated with all immunoconjugates did not show any pathological change (Fig. 7D).

The most important observation from a therapeutic standpoint was that only SUIT2-tumors treated with anti-collagen 4 immunoconjugate stopped growing about one month after treatment and remained dormant for more than 3 months. It may be concluded that the strategy of orchestrating slow sustained release from a scaffold erected on the stable inert structural components of the tumor stroma is most effective. We histologically compared this non-growing tumor with a size-matched, growing, control tumor and found that both tumors showed central necrosis due to decreased blood flow, which is often observed in a murine xenotransplant model [34,35]. The striking difference was that large confluent necrotic zones and dense fibrotic capsule formation

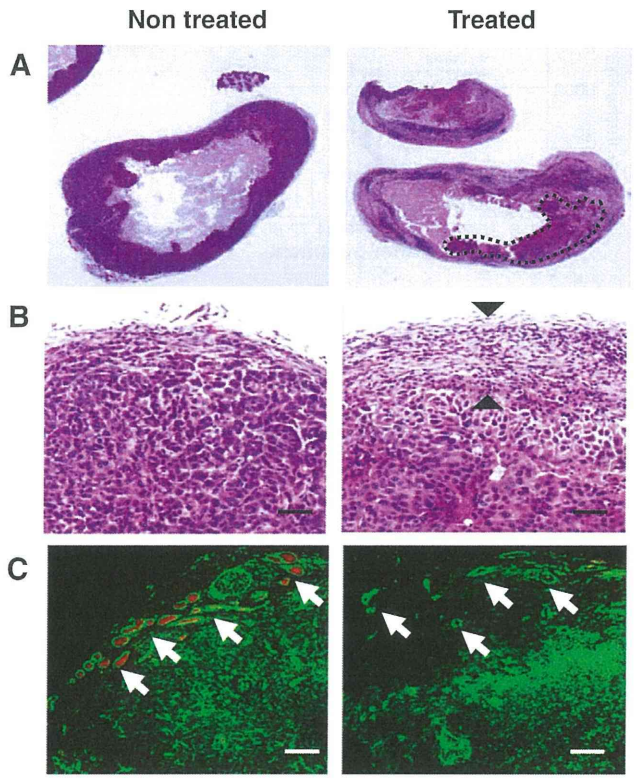

Fig. 8. Histopathological features of SUIT2 tumors after anti-collagen 4 immunoconjugate treatment. (A) Hematoxylin and eosin staining of non-treated (left) and immunoconjugate-treated (right) SUIT2-tumors. A non-necrotic viable lesion in the treated tumor is enclosed by a dotted line. (B) The fibrotic capsule width in the treated tumor is indicated between black arrowheads. (C) Tumor vessels were examined by the CD31 (red) collagen 4 (green) double-staining techniques. White arrows indicate tumor vessels or their traces in the boundary area. Scale bar: 100 μm [32].

were observed only in the treated tumor (Fig. 8A and B). In addition, CD31-positive endothelial cells, which may be tumor-feeding vessels in the peripheral part of the tumor, were never observed in the treated tumor compared with untreated control. Instead, many collagen 4-positive round profiles corresponding to traces of destroyed vessels were observed in the peripheral area of the treated tumor (Fig. 8C).

5.2. Anti-mouse (human) fibrin mAb conjugated with SN-38 in chemically induced tumor

Chemically induced mouse cutaneous cancer was selected as an appropriate experimental model for evaluating the therapeutic effects of our immunoconjugate chemotherapy, because this spontaneous carcinogenetic model has remarkable fibrin deposition and abundant interstitial tissue as in human cancer (Fig. 9A), unlike human tumor xenografts, which have less fibrin clots and interstitial tissue [36,37]. In addition, the spontaneous tumor is very slow in tumor growth that is also more similar to general human cancer as compared to the xenografts. Using systemic in vivo imaging, anti-fibrin IgM, anti-fibrin chimeric IgG and anti-fibrinogen IgG were delivered and retained in the tumor until Day 3, utilizing leaky tumor vessels [1–3]. However, accumulation of anti-fibrin IgM and anti-fibrinogen IgG was weak and was eliminated by Day 7, but the chimeric IgG was still highly retained (Fig. 9B). The use of human-chimera is benefit for clinical application to avoid human anti-mouse neutralizing antibodies (HAMA) and allergic reaction in human. In addition, because of the rapid blood clearance and low penetration of IgM compared with IgG [38], IgM is not suitable as a drug delivery vehicle. The branched composition had one maleimide for attachment of mAb, one PEG_{12} spacer and three PEG_{27} ester bonds for attachment of three SN-38 molecules (Fig. 10A). There were approximately eight thiol residues able to react with the maleimide in the reduced mAb. The calculated drug (SN-38)/mAb ratio of the immunoconjugate was about 24. This immunoconjugate exerted significantly stronger anti-tumor activity compared with CPT-11 (Fig. 10B). Although treatment-related body weight loss was observed in mice treated with each drug, there was no significant difference between control groups and CPT-11 or the immunoconjugate treatment group. After injection of the immunoconjugate, the concentration of total SN-38 (antibody bound and unbound form) and free SN-38 (unbound form) in plasma gradually declined within a week, whereas CPT-11 showed rapid clearance (Fig. 11A). Significantly high concentrations

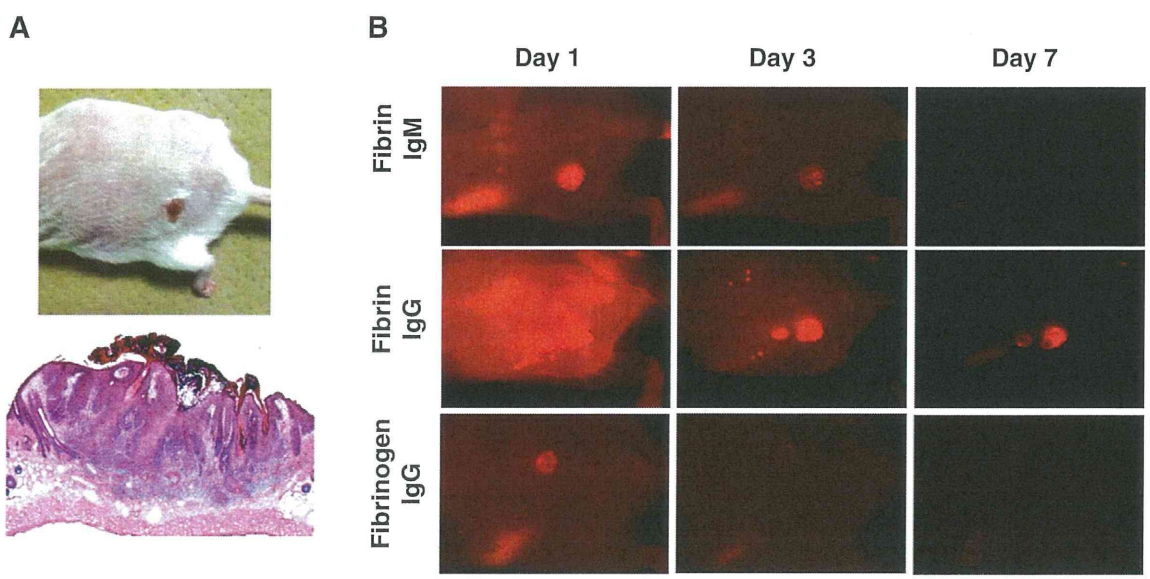

Fig. 9. In vivo systemic imaging analysis of Alexa-647-labeled anti-fibrin IgM, chimeric IgG or anti-fibrinogen mAb. (A) Chemically induced FVB/N mouse cutaneous tumor model. These spontaneous tumors have remarkable fibrin deposition and abundant interstitial tissue as in clinical human cancer,unlike human tumor xenografts in mice. (B) In vivo systemic imaging analysis of Alexa-647-labeled anti-fibrin IgM (upper), chimera IgG (middle) or anti-fibrinogen mAb (lower) on Days 1, 3 and 7 after injection. Arrows indicate each tumor position [29].

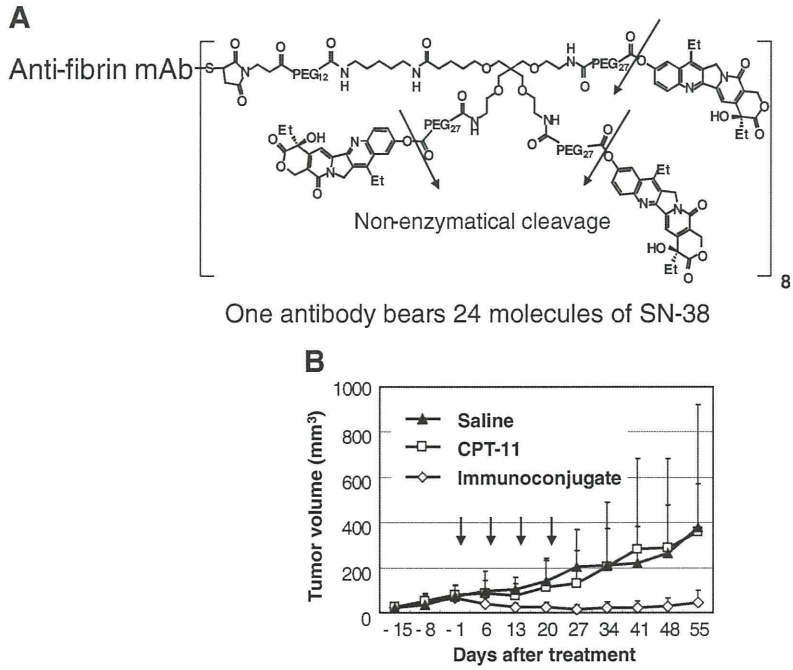

Fig. 10. Drug design and anti-tumor effect of anti-fibrin immunoconjugate. (A) Drug design of immunoconjugate; mAb-PEG-three branched PEG-$(SN\text{-}38)_3$ via ester bond. One antibody bears 24 molecules of SN-38. The arrow indicates the cleavage site for releasing free active SN-38. (B) Anti-tumor activity in vivo was examined. Immunoconjugates, CPT-11 or saline, were administered to mice bearing chemical-induced cutaneous cancer via intravenous injection on Day 0, 7, 14, and 21. Arrows indicate day of administration and the curves illustrate the effect of treatment on tumor size. $P = 0.0005$ (CPT-11 vs. immunoconjugate), $P < 0.0001$ (saline vs. immunoconjugate). Bar = SD [29].

of total and free SN-38 were detected in tumor tissues treated with the immunoconjugate for a long time compared to CPT-11 (Fig. 11B). The second significant observation of the treatment was a change in the gross tumor color from reddish to white (Fig. 11C). There was no clear change of fibroblast or macrophage, which play an important role for tumor progression [39,40]. It was found that discontinuation and irregularity comprising a mixture of narrowness and enlargement of the tumor vessels were manifested after treatment with the immunoconjugate (Fig. 12D and E).

6. Proposal of cancer stromal targeting (CAST) therapy and future prospects

Although there have been numerous reports of genetic and phenotype changes in tumors, a large body of pathological and clinical evidence indicates that there are no pivotal changes in tumor cells that distinguish them from normal dividing cells. Unlike in the case of using antibiotics against bacterial infection, therefore, ACAs need to be delivered selectively to tumor tissues and should be kept there long enough to reproduce the concentrations they reach in the Petri dish, which is a closed space where the cytocidal effects of any ACAs including molecular targeting agents are very strong. In the body, however, administered ACAs are cleared with the passage of time. Furthermore, as described in the main part of this topic, most human cancers possess abundant stroma that hinder the penetration of DDS including ACA-conjugated antibodies specific to surface antigens on cancer cells. I am now concerning that current studies mainly based on molecular and cellular biology while ignoring pathophysiology and pharmacology may be leading the development of antitumor drugs in the wrong direction. In our proof of concept studies using chemically induced spontaneous tumors (similar to general human cancers in terms of abundant tumor stroma and slow growing feature), we have made clear that our newly developed tool is not a simple cytotoxic immunoconjugate. Our strategic concept of cancer stromal targeting (CAST) therapy is unique as follows.

1) Newly developed cytotoxic immunoconjugate can extravasate from the leaky tumor vessels selectively, and forms a scaffold as it is captured by tumor stromal network.
2) The immunoconjugate allows the effective sustained release of anti-cancer agent from the scaffold, and this released anti-cancer agent is distributed throughout the tumor.
3) Consequently, the strategy described above was highly effective in causing arrest of tumor growth due to induced damage to tumor cells and tumor vessels without exerting the drug adverse effect (Fig. 12).

The present discovery by a hybrid of tumor stromal biology and physiology with organic chemistry may open a new field of drug design and produce many potentially useful treatment modalities especially for stromal rich and refractory cancer such as pancreatic cancer, stomach cancer, and glioma.

Disclosure statement

The author has no conflict of interest in this article.

Acknowledgements

This work was supported by the Third Term Comprehensive Control Research for Cancer from the Ministry of Health, Labour and Welfare of Japan (YM), the Japan Society for the Promotion of Science (JSPS) through the "Funding Program for World-Leading Innovative R&D on Science and Technology (FIRST Program)," initiated by the Council for Science and Technology Policy (CSTP) (YM), and National Cancer Center Research and Development Fund (YM).

I thank Drs. M. Yasunaga, S. Manabe and D. Tarin, for their scientific cooperation and discussion. I also thank Mrs. H. Koike and Mrs. M.

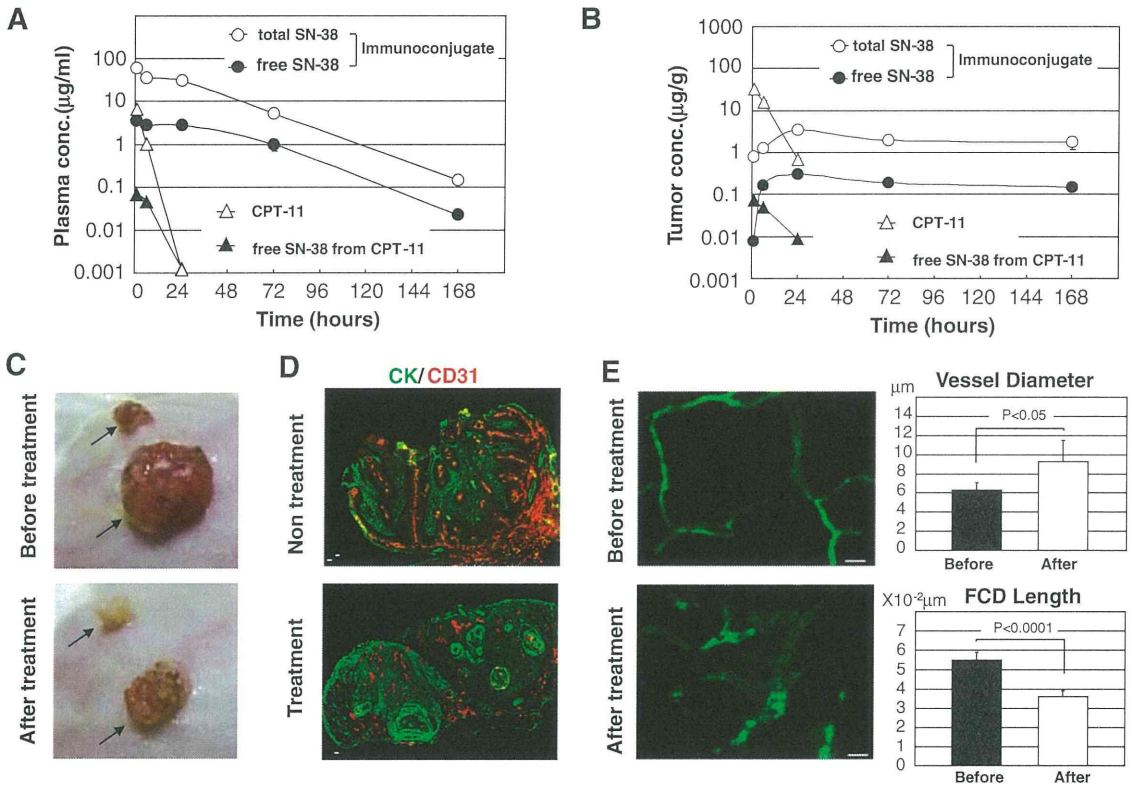

Fig. 11. Drug distribution and anti-vascular activity of the immunoconjugate. (A) Plasma concentration of total SN-38 (bound and unbound form) or CPT-11 and free SN-38 (unbound form) released from the immunoconjugate or converted from CPT-11 was determined using HPLC 1, 6, 24, 72, and 168 h after the injection. (B) Tumor concentration of total SN-38 (bound and unbound form) and free SN-38 (unbound form) released from the immunoconjugate, CPT-11 and free SN-38 converted from CPT-11 was determined. (C) Tumor color changed from reddish to white at 5 days after injection of the immunoconjugate but not CPT-11. Arrows indicate each tumor position. (D) Tumor vessels after the injection of the immunoconjugate were examined using CD31 (red) and CK (cytokeratin, green). Untreated mouse was used as control. Bar: 100 μm. (E) Tumor vessels before and after the injection were visualized using FITC-dextran by in vivo fibered confocal fluorescence microscopy (left). Quantified vessel diameter and functional capillary density (FCD) length are shown (right). Bar: 20 μm [29].

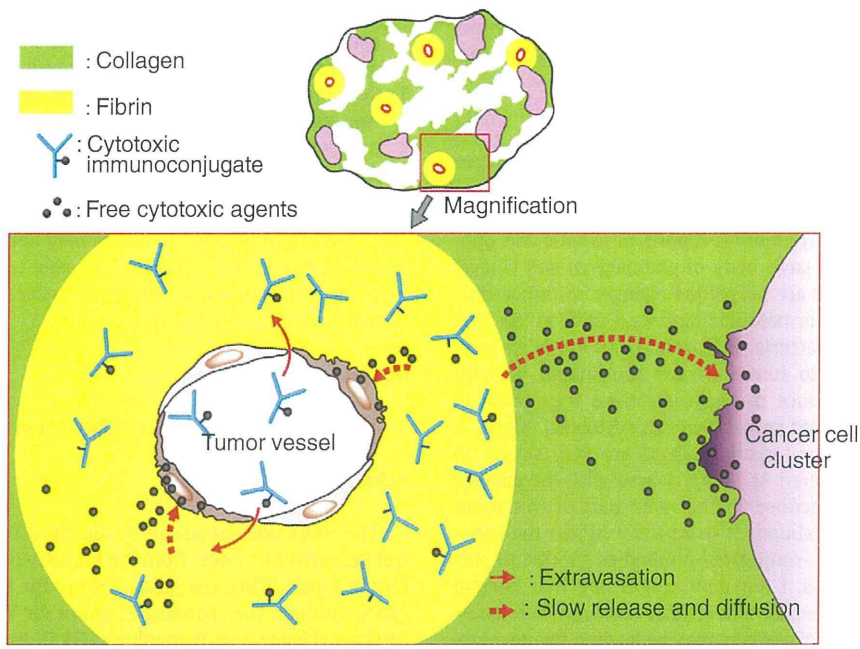

Fig. 12. New strategy of drug delivery using cytotoxic immunoconjugate directing tumor stroma in hypovascular and stroma-rich tumor. Newly developed immunoconjugates extravasate selectively from leaky tumor vessels, bind specifically to the fibrin network around the tumor vessels to create a scaffold, and then allow the effective sustained release of SN-38, a time-dependent anti-cancer agent, from the scaffold. Since this released anti-cancer agent is LMW, it is subsequently distributed over the entire tumor-stroma barrier and induces damage not only to tumor cells but also to tumor vessels [29].

Mizoguchi-Araake for helping me to establish the anti-fibrin mAb and Mrs. K. Shiina for preparation of this paper.

References

[1] Y. Matsumura, H. Maeda, A new concept for macromolecular therapeutics in cancer chemotherapy: mechanism of tumoritropic accumulation of proteins and the antitumor agent smancs, Cancer Res. 46 (1986) 6387–6392.
[2] R. Duncan, The dawning era of polymer therapeutics, Nat. Rev. 2 (2003) 347–360.
[3] H. Maeda, Y. Matsumura, EPR effect based drug design and clinical outlook for enhanced cancer chemotherapy, Adv. Drug Deliv. Rev. 63 (2011) 129–192.
[4] F.C. Courtice, The origin of lipoprotein in lymph, in: H.S. Meyersen (chairman), Lymph and the lymphatic system, C.C Thomas, Springfield, IL, 1963, pp. 89–126.
[5] K. Iwai, H. Maeda, T. Konno, Use of oily contrast medium for selective drug targeting to tumor: enhanced therapeutic effect and X-ray image, Cancer 44 (1984) 2115–2121.
[6] T. Tammela, K. Alitalo, Lymphangiogenesis: molecular mechanisms and future promise, Cell 140 (2010) 460–476.
[7] A.A. Gabison, Pegylated liposomal doxorubicin: metamorphosis of an old drug into a new form of chemotherapy, Cancer Invest. 19 (2001) 424–436.
[8] W.J. Gradishar, S. Tjulandin, N. Davidson, H. Shaw, N. Desai, P. Bhar, M. Hawkins, J. O'Shaughnessy, Phase III trial of nanoparticle albumin-bound paclitaxel compared with polyethylated castor oil-based paclitaxel in women with breast cancer, J. Clin. Oncol. 23 (2005) 7794–7803.
[9] Y. Matsumura, K. Kataoka, Preclinical and clinical studies of anticancer agent-incorporating polymer micelles, Cancer Sci. 100 (2009) 572–579.
[10] R. Duncan, Polymer conjugates as anticancer nanomedicines, Nat. Rev. Cancer 6 (2006) 688–701.
[11] D. Peer, J.M. Karp, S. Hong, O.C. Farokhzad, R. Margalit, R. Langer, Nanocarriers as an emerging platform for cancer therapy, Nat. Nanotechnol. 2 (2007) 751–760.
[12] T.M. Allen, Ligand-targeted therapeutics in anticancer therapy, Nat. Rev. 2 (2002) 750–759.
[13] S.O. Doronina, B.E. Toki, M.Y. Torgov, B.A. Mendelsohn, C.G. Cerveny, D.F. Chance, R.L. DeBlanc, R.P. Gearing, T.D. Bovee, C.B. Siegall, J.A. Francisco, A.F. Wahl, D.L. Meyer, P.D. Senter, Development of potent monoclonal antibody auristatin conjugates for cancer therapy, Nat. Biotechnol. 21 (2003) 778–784.
[14] A.M. Wu, P.D. Senter, Arming antibodies: prospects and challenges for immunoconjugates, Nat. Biotechnol. 23 (2005) 1137–1146.
[15] O. Trédan, C.M. Galmarini, K. Patel, I.F. Tannock, Drug resistance and the solid tumor microenvironment, J. Natl. Cancer Inst. 99 (2007) 1441–1454.
[16] C.M. Ghajar, M.J. Bissell, Extracellular matrix control of mammary gland morphogenesis and tumorigenesis: insights from imaging, Histochem. Cell Biol. 130 (2008) 1105–1118.
[17] A.I. Minchinton, I.F. Tannock, Drug penetration in solid tumors, Nat. Rev. Cancer 6 (2006) 583–592.
[18] H.F. Dvorak, Tumors: wounds that do not heal. Similarities between tumor stroma generation and wound healing, N. Engl. J. Med. 315 (1986) 1650–1659.
[19] A.D. Ricart, A.W. Tolcher, Technology insight: cytotoxic drug immunoconjugates for cancer therapy, Nat. Clin. Pract. Oncol. 4 (2007) 245–255.
[20] Y. Saito, M. Yasunaga, J. Kuroda, Y. Koga, Y. Matsumura, Enhanced distribution of NK012, a polymeric micelle-encapsulated SN-38, and sustained release of SN-38 within tumors can beat a hypovascular tumor, Cancer Sci. 99 (2008) 1258–1264.
[21] D. Mahadevan, D.D. Von Hoff, Tumor-stroma interactions in pancreatic ductal adenocarcinoma, Mol. Cancer Ther. 6 (2007) 1186–1197.
[22] H. Maeda, Y. Matsumura, H. Kato, Purification and identification of (hydroxyprolyl^3)-bradykinin in ascitic fluid from a patient with gastric cancer, J. Biol. Chem. 263 (1988) 16051–16054.
[23] Y. Matsumura, M. Kimura, T. Yamamoto, H. Maeda, Involvement of the kinin-generating cascade and enhanced vascular permeability in tumor tissue, Jpn. J. Cancer Res. 79 (1988) 1327–1334.
[24] D.R. Senger, S.J. Galli, A.M. Dvorak, C.A. Peruzzi, V.S. Harvey, H.F. Dvorak, Tumor cells secret a vascular permeability factor that promotes accumulation of ascites fluid, Science 219 (1983) 983–985.
[25] N. Ferrara, K.J. Hillan, H.P. Gerber, W. Novotny, Discovery and development of bevacizumab, an anti-VEGF antibody for treating cancer, Nat. Rev. Drug Discov. 3 (2004) 391–400.
[26] H.F. Dvorak, F.R. Rickles, Malignancy and hemostasis, in: R.W. Colman, V.J. Marder, A.W. Clowes, J.N. George, S.Z. Goldharber (Eds.), Hemostasis and Thrombosis: Basic principles and clinical practice, Fifth ed., LippinCott Williams & Wilkins, Philadelphia, 2006, pp. 851–873.
[27] A. Trousseau, Plegmasia alba dolens, Vol. 3, J.B. Balliere et Fils, Paris, 1865.
[28] P.D. Stein, A. Beemath, F.A. Meyers, E. Skaf, J. Sanchez, R.E. Olson, Incidence of venous thromboembolism in patients hospitalized with cancer, Am. J. Med. 119 (2006) 60–68.
[29] M. Yasunaga, S. Manabe, Y. Matsumura, New concept of cytotoxic immunoconjugate therapy targeting cancer-induced fibrin clots, Cancer Sci. 102 (2011) 1396–1402.
[30] E. Ostermann, P. Garin-Chesa, K.H. Heider, M. Kalat, H. Lamche, C. Puri, D. Kerjaschki, W.J. Rettig, G.R. Adolf, Effective immunoconjugate therapy in cancer models targeting a serine protease of tumor fibroblasts, Clin. Cancer Res. 14 (2008) 4584–4592.
[31] A. Palumbo, F. Hauler, P. Dziunycz, K. Schwager, A. Soltermann, F. Pretto, C. Alonso, G.F. Hofbauer, R.W. Boyle, D. Neri, A chemically modified antibody mediates complete eradication of tumours by selective disruption of tumour blood vessels, Br. J. Cancer 104 (2011) 1106–1115.
[32] M. Yasunaga, S. Manabe, D. Tarin, Y. Matsumura, Cancer-stromal targeting therapy by cytotoxic immunoconjugate bound to the collagen 4 network in the tumor tissue, Bioconjugate Chem. 22 (2011) 1776–1783.
[33] M.E. Davis, Z.G. Chen, D.M. Shin, Nanoparticle therapeutics: an emerging treatment modality for cancer, Nat. Rev. Drug Discov. 7 (2008) 771–782.
[34] S. Naito, A.C. von Eschenbach, I.J. Fidler, Different growth pattern and biologic behavior of human renal cell carcinoma implanted into different organs of nude mice, J. Natl. Cancer Inst. 78 (1987) 377–385.
[35] M.E. Fallowfield, Blood flow distribution within transplantable tumors in the mouse, Eur. J. Cancer Clin. Oncol. 25 (1989) 1683–1688.
[36] L.M. Ellis, I.J. Fidler, Finding the tumor copycat. Therapy fails, patients don't, Nat. Med. 16 (2010) 974–975.
[37] T. Hawighorst, P. Velasco, M. Streit, Y.K. Hong, T.R. Kyriakides, L.F. Brown, P. Bornstein, M. Detmar, Thrombospondin-2 plays a protective role in multistep carcinogenesis: a novel host anti-tumor defense mechanism, EMBO J. 20 (2001) 2631–2640.
[38] B.N. Rehlaender, M.J. Cho, Antibodies as carrier proteins, Pharm. Res. 15 (1998) 1652–1656.
[39] N.M. Bhowmick, E.G. Neilson, H.L. Moses, Stromal fibroblast in cancer initiation and progression, Nature 432 (2004) 332–337.
[40] G.K. Alderton, Tumor microenvironment: macrophages lead the way, Nat. Rev. Cancer 10 (2010) 162–163.

EUROPEAN JOURNAL OF CANCER 47 (2011) 2230–2239

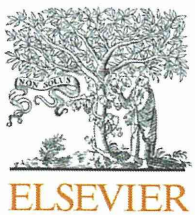

available at www.sciencedirect.com

ScienceDirect

journal homepage: www.ejconline.com

The inhibition of pancreatic cancer invasion-metastasis cascade in both cellular signal and blood coagulation cascade of tissue factor by its neutralisation antibody

Yohei Saito [a,b], *Yuki Hashimoto* [a,b], *Jun-ichiro Kuroda* [a], *Masahiro Yasunaga* [a], *Yoshikatsu Koga* [a], *Amane Takahashi* [a], *Yasuhiro Matsumura* [a,b,*]

[a] *Investigative Treatment Division, Research Center for Innovative Oncology, National Cancer Center Hospital East, 6-5-1 Kashiwanoha, Kashiwa, Chiba 277-8577, Japan*

[b] *Laboratory of Cancer Biology, Department of Integrated Biosciences, Graduate School of Frontier Sciences, The University of Tokyo, 5-1-5 Kashiwanoha, Kashiwa, Chiba 277-8562, Japan*

ARTICLE INFO

Article history:
Available online 27 May 2011

Keywords:
Pancreatic cancer
Tissue factor
Metastasis
Blood coagulation
Matrix metalloproteinase 9

ABSTRACT

Tissue factor (TF), the initiating cell surface receptor for the blood coagulation cascade, plays an important role in malignant transformation of the pancreas, although the precise mechanism remains unresolved. Here, we report that the TF – factor VIIa complex in human pancreatic cancer cells produced a significant amount of MMP-9 and promoted invasion ability *in vitro* and invasion and metastasis *in vivo*. For treatment, we successfully developed an anti-human TF monoclonal antibody that inhibits both cellular signalling and blood coagulation cascade via TF. Invasive capability and MMP-9 expression were significantly reduced by the antibody. The antibody inhibited not only tumour invasion in the orthotopic model, but also haematogenous metastasis in the portal-injection liver metastasis model. In conclusion, the TF-VIIa complex plays an important role in invasion-metastasis by enhancing tumour cell infiltration ability and forming microthrombi. The newly established anti-human TF neutralisation antibody may be useful for the treatment of pancreatic and other invasive cancers.

1. Introduction

In cancer invasion and metastasis, the cancer cells degrade the basement membrane and intravasate into lymphatic or blood microvessels. The cells are then transported to a new location and become clogged within the microvessels, proceeding to grow following extravasation.[1] These steps include cancer cell invasion, degradation of the basement membrane and stromal extracellular matrix (ECM), and formation of microthrombi. The matrix metalloproteinase (MMP) family represents important enzymes that degrade ECM and facilitate tumour invasion.[2] Amongst them, MMP-9 is well-known as one of the most important factors in facilitating invasion and metastasis in pancreatic cancer.[3]

Tissue factor (TF), the initiating cell surface receptor for the coagulation cascade, activates factor VIIa. The TF-VIIa complex activates factor X, and consequently this protease cascade forms fibrin clots.[4,5] The relationship between cancer and blood coagulation was initially described by the French surgeon Trousseau.[6] Cancer patients, especially those with pancreatic, stomach, and glioma cancer, often suffer from a state of hypercoagulation and venous thrombosis, leading to

* *Corresponding author:* at: Investigative Treatment Division, Research Center for Innovative Oncology, National Cancer Center Hospital East, 6-5-1 Kashiwanoha, Kashiwa, Chiba 277-8577, Japan. Tel./fax: +81 4 7134 6857.
E-mail address: yhmatsum@east.ncc.go.jp (Y. Matsumura).
0959-8049/$ - see front matter © 2011 Elsevier Ltd. All rights reserved.
doi:10.1016/j.ejca.2011.04.028

patient morbidity and mortality.[7–9] In another study using a fibrinogen-deficient transgenic mouse model, fibrinogen appeared to be an important element of the metastatic potential of circulating tumour cells.[10] Meanwhile, TF plays an important role in not only blood coagulation but also cell signalling in which the TF-VIIa complex phosphorylates extracellular-regulated kinase 1/2 (ERK1/2) via protease-activated receptor-2 (PAR-2).[11] Moreover, its complex promotes the expression of interleukin-8 (IL-8) and invasion in breast cancer cell lines.[12] However, the concrete involvement of TF in tumour invasion-metastasis has not yet been fully evaluated.

Human pancreatic cancer has one of the worst prognoses amongst cancers.[13] Invasion and metastasis advancing beyond the pancreas are typical. Direct invasion to nearby organs, such as the stomach, duodenum, colon, spleen and kidney frequently occurs. Distant metastasis to the liver and peritoneal dissemination are also commonly seen.[14,15] In terms of the relationship between TF and pancreatic cancer, TF expression is an important early event in malignant transformation of the pancreas.[16] TF expression may contribute to the aggressiveness of pancreatic cancer that would stimulate tumour invasiveness, and evaluation of the primary tumour for TF expression may identify patients with a poor prognosis.[17,18]

Therefore, elucidation of the relationship between TF and pancreatic cancer invasion-metastasis may lead to the development of new therapeutic strategies as well as a better understanding of pancreatic cancer biology.

2. Materials and methods

2.1. *Cell lines*

Human pancreatic cancer cell lines BxPC3, Panc1, Capan1, and MIA PaCa-2 were purchased from the American Type Culture Collection (Rockville, MD, USA). The cell lines were maintained in Dulbecco's Modified Eagle's Medium supplemented with 10% faetal bovine serum (FBS) (Cell Culture Technologies, Gaggenau-Hoerden, Germany), 100 units/mL streptomycin, and 2 mmol/L L-glutamine (Sigma, St. Louis, MO, USA) in an atmosphere of 5% CO_2 at 37 °C.

2.2. *Immunocytochemistry*

Cells (1×10^5) were seeded on a 4-well culture slide (BD Biosciences, Bedford, MA, USA), which was incubated for 24 h at 37 °C. Then, after removal of the medium, the sections were rinsed with phosphate buffered saline (PBS) and soaked in 4% paraformaldehyde phosphate buffer solution for 15 min. The sections were then rinsed with PBS, and endogenous peroxidase activity was blocked with a 0.3% hydrogen peroxide solution in 100% methanol for 20 min. After the sections were rinsed with PBS three times for 5 min each, non-specific protein binding was blocked with 5% skim milk (BD, Franklin Lakes, NJ, USA) in PBS for 30 min at room temperature, followed by washing three times with PBS for 5 min. A mouse monoclonal antibody against human TF (Calbiochem, La Jolla, CA, USA) or a rat monoclonal antibody against human TF (established by USA) named as 1849 was added, incubated for 1 h, and rinsed three times with PBS for 5 min each. The sections were incubated for 30 min with EnVision™/HRP (Dako, Glostrup, Denmark) directed against each primary antibody. The sections were rinsed three times with PBS and incubated using the DAB+(3,3-diaminobenzidine tetrahydrochloride) Liquid System (Dako, Glostrup, Denmark) for 30 s. Finally, the sections were rinsed with water and counterstained with haematoxylin solution.

2.3. *Immunohistochemistry*

10^7 cells of each pancreatic cancer cell line were injected subcutaneously in 4-week-old female BALB/c nude mice. When the tumour volume reached 300 mm^3, tumours were excised from the mice under anaesthetic. Immunohistochemical analysis was conducted as described previously.[19] As a primary antibody, we used the rat monoclonal antibody against human TF that we created. In addition, we used goat anti-rat IgG/HRP (Jackson ImmunoResearch Laboratories, West Grove, PA, USA) as a secondary antibody.

2.4. *Transfection of BxPC3 cells with TF short hairpin RNA (TF shRNA), green fluorescent protein (GFP), and luciferase*

Lentiviral particles were purchased from Sigma–Aldrich. BxPC3 cell suspension (1000 cells/100 μL) was seeded on a 96-well plate, which was incubated for 24 h at 37 °C. After removal of the medium, 100 μL of medium containing hexadimethrine bromide (final concentration of 8 μg/ml) was added to the cells. Viral particles carrying TF shRNA or non-target shRNA (multiplicity of infection (MOI) = 20) were added to the cells. After selecting the infected cells using 2 μg/ml puromycin, we established a TF-knockdown cell line (BxPC3 TFshRNA) and a control cell line (BxPC3 mock). For the detection of micrometastasis and microinvasion in pancreatic orthotopic tumour xenografts, both BxPC3 mock and BxPC3 TFshRNA were infected with viral particles carrying GFP (MOI = 20). In addition, the BxPC3 cell line stably expressing firefly luciferase and YFP mutant Venus ($BxPC3^{Luc}$) was established. In brief, the coding sequence for firefly luciferase and Venus was subcloned into the pIRES vector (Clontech Laboratories, Mountain View, CA, USA). The fragment consists of Luciferase-IRES-Venus generated from the plasmid with the restriction enzymes Nhe1 and Not1. This fragment was subcloned into the pEF6/V5-His vector (Invitrogen, Carlsbad, CA, USA) to generate plasmids of pEF6-Luciferase IRES Venus. BxPC3 were seeded on 6-well plate 24 h before transfection. The cells were transfected with pEF6-Luciferase IRES Venus using Lipofectamine™ LTX with Plus™ Reagent (Invitrogen) according to the manufacturer's instructions, and then incubated for 48 h at 37 °C. The cells were then passaged in medium containing blasticidin (10 μg/ml; InvivoGen, San Diego, CA, USA) to select the blasticidin resistance gene integrated in the pEF6/V5-His plasmids.

2.5. *Real-time PCR analysis for MMPs and TF*

Total RNA was extracted from pancreatic cancer cell lines using the RNeasy Mini Kit (Qiagen, Valencia, CA, USA) according to the manufacturer's instructions. cDNA was synthesised from total RNA using the High Capacity cDNA Reverse Transcription Kit (Applied Biosystems, Foster City, CA, USA) in accordance with